Nonweak-Coupling Regge Trajectories from Field-Theory Models*

ARTHUR R. SWIFT AND ROBIN W. TUCKER
Department of Physics and Astronomy, University of Massachusetts, Amherst, Massachusetts 01002
(Received 26 January 1970)

Perturbation-theory techniques are used to generate an approximate transcendental equation for the leading Regge pole produced by an infinite sum of Feynman ladder diagrams. This equation is not restricted to the weak-coupling domain and can be used to produce trajectories with $\alpha(0)>0$. The equation is solved both below and above the elastic and inelastic thresholds to provide the first complete description of a relativistic Regge trajectory in the ladder-diagram model. The same technique is used to generate potential-theory trajectories which agree with the exact solutions obtained by more complicated methods.

I. INTRODUCTION

In the past few years the concept of a Regge pole has played a very important role in both the interpretation of high-energy scattering experiments and in the classification of many of the hadronic resonances discovered at lower energies. In spite of the phenomenological success of Regge poles, there does not exist at this time a firm theoretical understanding of the mechanisms by which they are generated in intrinsically relativistic processes. Regge poles have been intensively investigated in potential theory[1] and, in fact, potential theory constitutes the only complete theory of Regge poles. However, because of the absence of such relativistic phenomena as multiple thresholds, cuts, and daughter poles, the utility of potential theory as a guide to the nature of Regge poles in a relativistic world is questionable.

Since there does not exist a complete relativistic theory of strongly interacting particles, it is recognized that valuable insight into the properties of real Regge trajectories can be obtained by studying simple models that embody certain aspects of the complete problem. Such models can be divided into two main classes. There are S-matrix models which usually assume the existence of Regge poles and generate constraints on their behavior through the use of crossing, unitarity, duality, and so forth.[2] The second class of models is based on field theory; a fundamental interaction is assumed and Regge poles are dynamically generated either by summing diagrams with perturbation-theory techniques[3,4] or by solving the Bethe-Salpeter equation.[5,6] Although both S-matrix and field-theory models are useful, field-theory models, though more unrealistic, are more fundamental in the sense that they provide a dynamical mechanism for the appearance of Regge poles. For those who would argue that the multiperipheral model or its generalizations are a fundamental theory of Regge poles, we point out that the multiperipheral equation in its original form is mathematically identical to the Bethe-Salpeter equation.[7] Thus, all work on field-theory models can be couched in the more fashionable language of the multiperipheral model, but we prefer to retain the more familiar ideas and language of field theory while keeping in mind the possibility of translation.

The simplest field-theory model of a Regge pole uses an infinite sum of ladder Feynman diagrams where all internal particles have zero spin.[3,4] The ladder approximation to the Bethe-Salpeter equation is one way of representing this sum. This formidable integral equation can be solved either in the weak-coupling limit or numerically for arbitrary coupling.[6] The numerical solutions are difficult to obtain and have never been extended above the two-particle threshold. The trajectories obtained from ladder diagrams by perturbation theory have been extensively investigated only in the weak-coupling limit where the leading pole is given by $\alpha+1=G^2K(s)$,[3] G being the coupling constant. Perturbation-theory solutions, however, have the virtue of yielding relatively simple analytic expressions for the trajectories. Polkinghorne[4] showed that through the use of Mellin transforms it is possible to obtain an exact equation for the leading Regge pole that has the form $\alpha+1=F(\alpha,s)$. The Regge trajectory $\alpha(s)$ is the solution of this transcendental equation, and $F(\alpha,s)$ is given by a power series in the coupling constant. The coefficient of G^{2N} is a $(3N-1)$-dimensional integral over Feynman parameters. As a result of this complexity, this exact equation has not been used to generate explicit trajectories. By keeping only the lowest term in the series for $F(\alpha,s)$, Polkinghorne[4] apparently obtains weak-coupling trajectories near the threshold energy where $\alpha(s)\approx-\frac{1}{2}$. However, his threshold solution is not unique. It depends crucially on the dependence of the first-order term in his expression for $F(\alpha,s)$. The very nature of a perturbation expansion for the trajectory function implies that this α dependence is

* Supported in part by the National Science Foundation.

[1] A complete description of Regge poles in potential theory is found in R. G. Newton, *The Complex j-Plane* (Benjamin, New York, 1964).

[2] R. Dolen, D. Horn, and C. Schmid, Phys. Rev. Letters **19**, 402 (1967); M. Ademollo, H. Rubinstein, G. Veneziano, and M. Virasoro, Phys. Rev. **176**, 1904 (1968); G. Veneziano, Nuovo Cimento **57A**, 190 (1968); G. F. Chew, M. L. Goldberger, and F. E. Low, Phys. Rev. Letters **22**, 208 (1969); G. F. Chew and A. Pignotti, Phys. Rev. **176**, 2112 (1968).

[3] R. J. Eden, P. V. Landshoff, D. I. Olive, and J. C. Polkinghorne, *The Analytic S-Matrix* (Cambridge U. P., Cambridge, England, 1966), Chap. 3. References to most of the early work on perturbation theory can be found in this book.

[4] J. C. Polkinghorne, J. Math. Phys. **5**, 431 (1964). This paper will be referred to as P.

[5] B. W. Lee and R. F. Sawyer, Phys. Rev. **127**, 2266 (1962); R. R. Sawyer, *ibid.* **131**, 1384 (1963).

[6] V. Chung and D. R. Snider, Phys. Rev. **162**, 1629 (1967); R. E. Cutkosky and B. B. Deo, Phys. Rev. Letters **19**, 1256 (1967).

[7] D. Amati, A. Stanghellini, and S. Fubini, Nuovo Cimento **26**, 6 (1962); B. W. Lee and A. R. Swift, *ibid.* **27**, 1272 (1963).

not unique but rather represents a judicious sampling of higher-order terms.

In this paper we present an approximate, but nonperturbative, method of solving the exact equation obtained by Polkinghorne. From perturbation theory we calculate Regge trajectories which are not restricted to the weak-coupling domain and, moreover, can be analytically continued above threshold to obtain the first complete description of the trajectories in the complex angular momentum plane for a relativistic field-theory model. The final equation we obtain retains much of the simplicity of perturbation-theory models. Our technique can equally well be applied to potential theory, where it is possible to compare it with exact solutions[8] in order to test its validity. The basic approach is to exploit the formal similarity between the expression for $F(\alpha, s)$ and an infinite sum of ladder diagrams with contracted ends. We construct a set of Feynman rules which enable us to write an integral equation for $F(\alpha, s)$. The kernel of the equation is approximated by one of finite rank. The first approximation with just a single separable kernel turns out to be surprisingly good, both when compared with the second approximation and when compared with the exact results available for nonrelativistic Regge trajectories. Since our method yields a simple transcendental equation that is valid both for strong couplings and for energies above threshold, it should provide a useful technique for investigating, among other things, the properties of daughter poles and cuts in a domain previously unexplored.

We start in the next section with a development of the basic theory. Nonrelativistic and relativistic scattering are developed simultaneously with Polkinghorne's exact equation for the leading Regge trajectory as the starting point. In the final section the equations are solved in the first and second approximations and compared with exact solutions where available. The behavior of the relativistic trajectory is discussed. As an example of the usefulness of our approach we solve for the leading Regge trajectory in a model with multiple thresholds. The limitations of the method are discussed, and other applications are suggested.

II. THEORY

We start with the exact equation for the leading Regge pole obtained from an infinite sum of ladder diagrams:

$$\alpha(s)+1=F(\alpha(s), s), \tag{1}$$

where $F(\alpha, s)$ is given by

$$F(\alpha, s)=-\sum_{N=0}^{\infty}(-G^2)^{N+1}\int_0^{\infty}\prod_{i=1}^{N+1}dy_i dz_i \times\prod_{j=1}^{N}dx_j\frac{x_j^{\alpha+1}-1}{\alpha+1}\frac{\partial}{\partial x_j}\left(\frac{e^{-Q_N}}{\Delta_N{}^{\alpha+2}}\right) \tag{2}$$

and $G^2=g^2/16\pi^2$ in the notation of P.[4] The rungs of the ladders carry mass λ, and the corresponding Feynman parameters are x_i. The parameters for the sides of the ladder carrying mass μ are y_i and z_i. The functions Q_N and Δ_N are defined in P and describe an N-rung ladder with both ends contracted. In nonrelativistic scattering from a Yukawa potential, the leading pole is given by (1) with only a slight change in the form of $F(\alpha, s)$ to take into account the fact that the ladders are one-sided and the space is three rather than four dimensional.[9] Thus, G^2 becomes $g/2\sqrt{\pi}$, where

$$V(r)=-g(e^{-\lambda r}/r).$$

The Feynman parameter z_i is absent; Δ_N is derived from the relativistic Δ_N by setting $z_i=0$; and $\Delta_N{}^{-(\alpha+2)}$ is replaced by $\Delta_N{}^{-(\alpha+3/2)}$. The expression for Q_N is given in Ref. 9. Since the solutions of (1) generate trajectories which lie to the right of $\mathrm{Re}\alpha=-1$ in the complex angular momentum plane, the derivatives with respect to x_i can be removed from (2) by integration by parts to give

$$F(\alpha, s)=\frac{\bar{F}(\alpha, s)}{1+\bar{F}(\alpha, s)/(\alpha+1)}, \tag{3}$$

where

$$\bar{F}(\alpha, s)=\sum_{N=0}^{\infty}(G^2)^{N+1}\int_0^{\infty}\prod_{i=1}^{N+1}dy_i dz_i\prod_{j=1}^{N}dx_j x_j{}^{\alpha}\frac{e^{-Q_N}}{\Delta_N{}^{\alpha+2}}. \tag{4}$$

At a pole of $\bar{F}(\alpha, s)$, $F(\alpha, s)=\alpha+1$, so that the problem of solving (1) reduces to the problem of finding the pole of $\bar{F}(\alpha, s)$. If α is set equal to zero in (4), $\bar{F}(0, s)$ is identically the expression for an infinite sum of contracted ladder diagrams with four-dimensional loop integrations over internal momenta. If we replace the normal propagator $(p^2+\lambda^2)^{-1}$ by

$$\Gamma(\alpha+1)/(p^2+\lambda^2)^{\alpha+1},$$

where $\Gamma(z)$ is the gamma function, this sum of contracted ladders would yield (4) (including the $x_i{}^{\alpha}$) with $\Delta_N{}^{-2}$ instead of $\Delta_N{}^{-(\alpha+2)}$. The power of Δ_N is tied to the dimensionality of the loop integrations. In other words, if instead of a four-dimensional space, we had an L-dimensional space, we would find $\Delta_N{}^{-L/2}$. Thus, $\bar{F}(\alpha, s)$ represents the sum of contracted ladder diagrams in an L-dimensional space with L equal to $2(\alpha+2)$ and the propagator given by the above expression. In what follows we use this set of formal Feynman rules to replace (3) by an equivalent expression involving loop integrations. The admittedly heuristic step of working in a $(2\alpha+4)$-dimensional space is justified on the grounds that the results so obtained are reasonable and agree with other methods of solving the same problem. The loop integrations in a $(2\alpha+4)$-dimensional space where α is an arbitrary complex number are to be under-

[8] C. Lovelace and D. Messon, Nuovo Cimento **26**, 472 (1962).

[9] A. R. Swift, Phys. Rev. **176**, 1848 (1968).

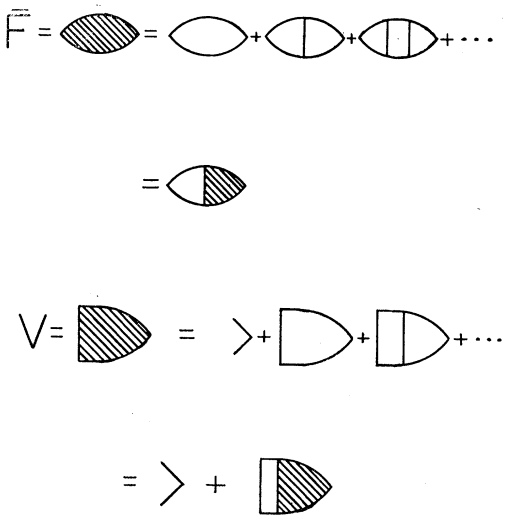

Fig. 1 Steps involved in going from the infinite-sum representation of $\bar{F}$ to the integral equation for V shown diagrammatically. Each Feynman diagram is computed using the Feynman rules developed in the text.

stood as first being carried out in an L-dimensional space, L an arbitrary positive integer; then L is replaced by $2\alpha+4$.

With the additional restriction of a Euclidean metric, $\bar{F}(\alpha, s)$ can be written in the form

$$\bar{F}(\alpha, s)=\frac{G^2}{(\pi)^{\alpha+2}}\int\frac{d^{2\alpha+4}k\ V(\alpha, s, k)}{[(k+iE)^2+\mu^2][(k-iE)^2+\mu^2]}, \tag{5}$$

where E is a vector in the k_0 direction in an L-dimensional space and $E^2=\frac{1}{4}s$. The function $V(\alpha, s, k)$ represents an infinite sum of ladders with one end contracted; and, just as the amplitude which is a sum of conventional ladders satisfies an integral equation, $V(\alpha, s, k)$ satisfies the equation

$$V(\alpha, s, k)=1+\frac{G^2}{\pi^{\alpha+2}}\times\int\frac{d^{2\alpha+4}q\ \Gamma(\alpha+1)\,V(\alpha, s, q)}{[(k-q)^2+\lambda^2]^{\alpha+1}[(q+iE)^2+\mu^2][(q-iE)^2+\mu^2]}. \tag{6}$$

The steps involved in going from (4) to (6) are shown diagrammatically in Fig. 1. Clearly the poles of $\bar{F}(\alpha, s)$ are also the poles of $V(\alpha, s, k)$. The problem of solving for the leading trajectory becomes one of solving (6), which, except for the α dependence of the kernel, is essentially the Bethe-Salpeter equation. The steps leading to (6) can be repeated for the nonrelativistic problem and yield

$$V_P(\alpha, s, k)=1+\frac{g/2\sqrt{\pi}}{\pi^{\alpha+3/2}}\int\frac{d^{2\alpha+3}q\ \Gamma(\alpha+1)\,V_P(\alpha, s, q)}{[(k-q)^2+\lambda^2]^{\alpha+1}(q^2-s)}. \tag{7}$$

In this case $\sqrt{s}$ is the nonrelativistic energy. The momentum integration has one less dimension than in the relativistic case, as is expected.

Equations (6) and (7) do not lend themselves readily to numerical solution owing to the presence of the $(2\alpha+4)$-dimensional integration. Moreover, direct numerical solution of these equations would encounter the same problem of continuation above threshold that afflicts work on the Bethe-Salpeter equation. Rather, we approximate the kernel of (6) or (7) by one of finite rank as a method of obtaining nonperturbative solutions. We expand the kernel in the following way:

$$\left(\frac{1}{(p-k)^2+\lambda^2}\right)^{\alpha+1}=\frac{(\lambda^2)^{\alpha+1}}{(p^2+\lambda^2)^{\alpha+1}(k^2+\lambda^2)^{\alpha+1}}\times[(1-B)^{-(\alpha+1)}]$$
$$=\frac{(\lambda^2)^{\alpha+1}}{(p^2+\lambda^2)^{\alpha+1}(k^2+\lambda^2)^{\alpha+1}}\times[1+(\alpha+1)B+\cdots], \tag{8}$$

where $B=(p^2k^2+2\lambda^2p\cdot k)/(p^2+\lambda^2)(k^2+\lambda^2)$. This approximation to the kernel has been used before in similar situations and matches well the form of the exact kernel when p^2 or k^2 separately become large. Keeping just the first term in (8), we find that

$$V(\alpha, s, k)=1+[G^2\Gamma(\alpha+1)(\lambda^2)^{\alpha+1}/(k^2+\lambda^2)^{\alpha+1}]C. \tag{9}$$

The constant C is given by

$$C=K(\alpha+1)/[1-G^2\Gamma(\alpha+1)(\lambda^2)^{\alpha+1}K(2\alpha+2)]. \tag{10}$$

The function $K(\beta)$ is defined by

$$K(\beta)=\frac{1}{\pi^{\alpha+2}}\int\frac{d^{2\alpha+4}k}{(k^2+\lambda^2)^{\beta}[(k+iE)^2+\mu^2][(k-iE)^2+\mu^2]}. \tag{11}$$

If the propagators are written in exponential form by use of Feynman parameters, the k integration is easily carried out. The corresponding potential-theory solution is the same, except that

$$K_P(\beta)=(1/\pi^{\alpha+3/2})\int[d^{2\alpha+3}k/(k^2+\lambda^2)^{\beta}(k^2-s)]. \tag{12}$$

Since the poles of C are the poles of $V(\alpha, s, k)$, the leading Regge trajectory in this approximation is the solution of the simple transcendental equation

$$1=G^2\Gamma(\alpha+1)(\lambda^2)^{\alpha+1}K(2\alpha+2). \tag{13}$$

Note that (13) is scale invariant. If every mass, energy, and coupling constant is scaled by $s_0^{1/2}$, the dependence cancels out completely. This is an important property of the exact equation (1) and means that the energy scale is set by the masses in the problem and is not arbitrary. Not all approximations to (1) have this property.

If the next approximation to the kernel in (8) is retained, $V(\alpha, s, k)$ is found to have the form

$$V(\alpha, s, k)=1+[C_1/(k^2+\lambda^2)^{\alpha+1}]+[C_2/(k^2+\lambda^2)^{\alpha+2}].$$

C_1 and C_2 have poles given by the equation

$$1=G^2\Gamma(\alpha+1)(\lambda^2)^{\alpha+1}K(2\alpha+2)$$
$$+G^2\Gamma(\alpha+2)(\lambda^2)^{\alpha+1}[K(2\alpha+2)-2\lambda^2K(2\alpha+3)$$
$$+\lambda^4K(2\alpha+4)]-G^4\Gamma(\alpha+1)\Gamma(\alpha+2)(\lambda^2)^{2\alpha+4}$$
$$\times[K(2\alpha+2)K(2\alpha+4)-K(2\alpha+3)^2]. \quad (14)$$

The $p\cdot k$ term in (8) does not contribute to this order. Both (13) and (14) reduce to the well-known weak-coupling solutions when G^2 is small and $\alpha\to-1$. In Sec. III we solve (13) and (14) and show that the second approximation differs only slightly from the first approximation, but in the right direction to improve the agreement with the exact solutions.

If (6) is solved with Fredholm theory instead of with the finite rank approximation, the poles of $V(\alpha, s, k)$ come from the vanishing of the Fredholm denominator. In lowest order the position of the pole is just that obtained in first order from (1). Explicit calculation shows that this first-order term is proportional to $\Gamma(-\alpha)$. The pole of the gamma function at $\alpha=0$ makes it impossible to generate trajectories which rise above

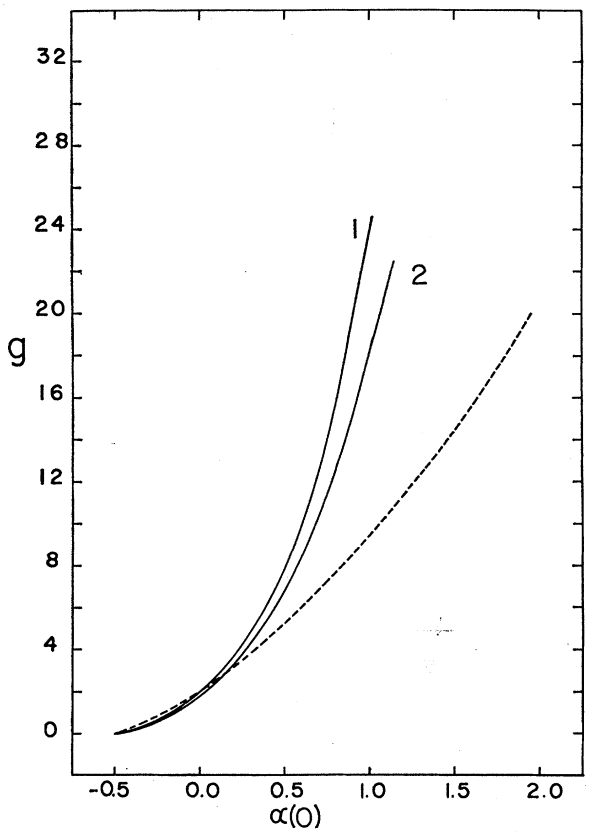

FIG. 2. Position of the leading Regge trajectory at $s=k^2=0$ in potential theory shown as a function of g, the strength of the potential. The range of the potential is set equal to 1. The curves labelled 1 and 2 are the first and second approximations developed in the text, while the dashed curve is from the exact solutions of Lovelace and Masson (Ref. 8).

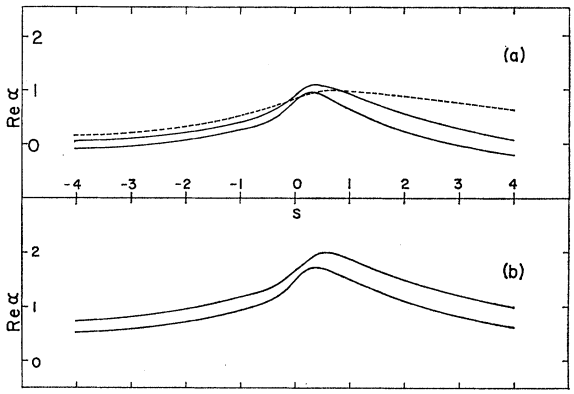

FIG. 3. Reα plotted as a function of s for the potential-theory trajectories obtained in either the first or second approximations. In (a), $G^2=g/2\sqrt{\pi}=4.0$, while $G^2=16.0$ in (b). In both (a) and (b) the lower of the two solid curves represents the first approximation and the upper is the second approximation. The dashed curve is the exact trajectory calculated by Lovelace and Masson (Ref. 8) for $G^2=2.0$. The range of the potential is the same as in Fig. 2.

$\alpha=0$. Presumably this pole is cancelled by higher-order terms. In any case our method of approximation avoids this difficulty. A second point to notice is that (13) and (14) are unaffected by the possibility of replacing $x^{\alpha+1}-1$ by $x^{\alpha+1}-f(\alpha)$ in (2), where $f(\alpha)$ is an arbitrary function of α and the Feynman parameters satisfying $f(-1)=1$.[10] The freedom in choice of $f(\alpha)$ affects only the ends of the Feynman-diagram representation of $\bar{F}(\alpha, s)$ [see Eq. (4)] and does not change the kernel of the integral equation for $V(\alpha, s, k)$.

III. RESULTS AND DISCUSSION

In order to extract trajectories from (13) or (14), we write the propagators in exponential form and perform the k integration in $K(\beta)$ to obtain

$$K(\beta)=[\Gamma(\beta)]^{-1}$$
$$\times\int_0^\infty \frac{dxdydz\ x^{\beta-1}\exp[-\lambda^2x-\mu^2(y+z)+\frac{1}{4}sQ]}{(x+y+z)^{\alpha+2}}, \quad (15)$$

where $(x+y+z)Q=x(y+z)+4yz$. Using standard scaling transformations, we convert the three-dimensional integral in (15) to the form

$$K(\beta)=\frac{\Gamma(\beta-\alpha)}{\Gamma(\beta)}\int_0^1 dx\,x^{\beta-1}(1-x)\int_0^1 dy\,\frac{1}{M^{\beta-\alpha}}, \quad (16)$$

with $M=\lambda^2x+\mu^2(1-x)-\frac{1}{4}s[x(1-x)+4(1-x)^2y(1-y)]$. The corresponding expression for potential theory is

$$K_P(\beta)=\frac{\Gamma(\beta-\alpha-\frac{1}{2})}{\Gamma(\beta)}\int_0^1\frac{dx\,x^{\beta-1}}{M_P^{\beta-\alpha-1/2}}, \quad (17)$$

where $M_P=\lambda^2x-s(1-x)$. $K_P(\beta)$ is proportional to a hypergeometric function. The integral representations of $K(\beta)$ and $K_P(\beta)$ in (16) and (17) are convergent

[10] For a discussion of the ambiguity in summing ladder diagrams, see Ref. 9.

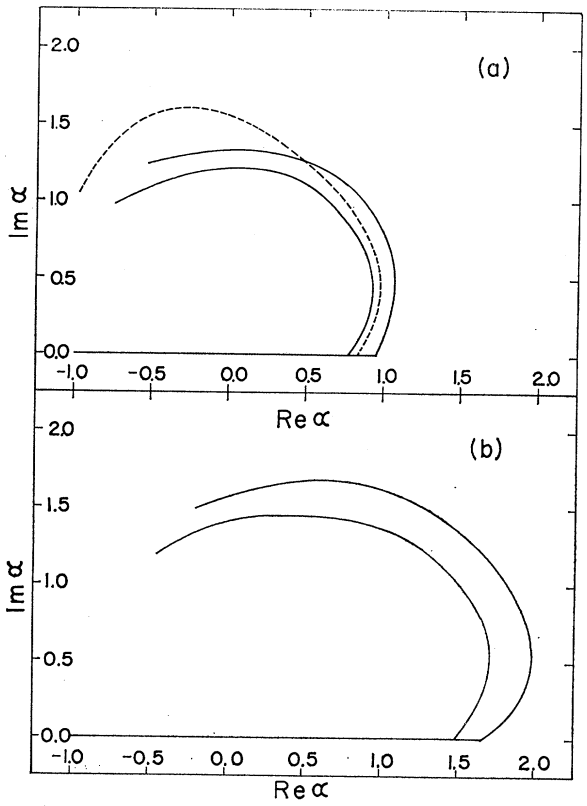

FIG. 4. The trajectories plotted in Fig. 3 are shown in the complex α plane. Again $G^2=4.0$ in (a) and 16.0 in (b), and the two solid curves are the first and second approximations. The dashed curve is the exact trajectory for $G^2=2.0$.

for s below the elastic threshold. [The elastic thresholds are at $s=4\mu^2$ in (16) and at $s=0$ in (17).] For $s>4\mu^2$, the singularities of (16) are most conveniently exposed by a further change of variables to $y=\frac{1}{2}(1+u^{1/2})$, $x=1-w$, and $s=4(\mu^2+\Delta)$ so that

$$K(\beta)=\frac{\Gamma(\beta-\alpha)}{\Gamma(\beta)}\frac{1}{2}\int_0^1 dw(1-w)^{\beta-1}w \times\int_0^1\frac{du}{\sqrt{u}}[M(u,w)]^{\alpha-\beta}, \quad (16')$$

where $M(u,w)=\lambda^2(1-w)-\Delta w(1-wu)+\mu^2uw^2$. As the energy is increased, the curve $M(u,w)=0$ moves into the region of integration when Δ becomes positive. This produces the elastic threshold. For $0<\Delta<\lambda^2+2\lambda\mu$, the curve $M(u,w)=0$ cuts the boundary of the region of integration at $u=0$, $w=\lambda^2/(\lambda^2+\Delta)$ and at $w=1$, $u=\Delta/(\mu^2+\Delta)$. However, for $\Delta>\lambda^2+2\lambda\mu$ the curve also cuts the $u=1$ boundary twice. This introduces a second threshold singularity at $s=4(\lambda+\mu)^2$. This four-particle threshold presumably reflects the higher thresholds contained in the integral equation (6). The representation (16') is contained above the first threshold by separating the region of integration in which M is negative and using the fact that s has a $+i\epsilon$ attached to it. This allows us to write $M^{\beta-\alpha}=\exp[-i\pi(\beta-\alpha)](-M)^{\beta-\alpha}$. The correct continuation of $K(\beta)$ for $4\mu^2<s<4(\lambda+\mu)^2$ is

$$K(\beta)=\tfrac{1}{2}\pi^{3/2}\frac{\Delta^{\alpha+1/2}}{\Gamma(\alpha+\frac{3}{2})}\frac{i-\tan\pi\alpha}{(\lambda^2+\Delta)^\beta(\mu^2+\Delta)^{1/2}} -\tfrac{1}{2}\pi^{1/2}\frac{\Gamma(\beta-\alpha-\frac{3}{2})}{\Gamma(\beta)}\frac{F(1-\beta,1;\frac{5}{2}+\alpha-\beta;\lambda^2/(\lambda^2+\Delta))}{(\lambda^2+\Delta)(\mu^2+\Delta)^{1/2}(\lambda^2)^{\beta-\alpha-3/2}} -\frac{1}{2}\frac{\Gamma(\beta-\alpha)}{\Gamma(\beta)}\int_0^1 dw(1-w)^{\beta-1}w\int_0^1\frac{dx\,x^{\beta-\alpha-3/2}}{(M')^{\beta-\alpha}}, \quad (18)$$

where $F(a,b;c;z)$ is a hypergeometric function and $M'=(\mu^2+\Delta)w^2+x[\lambda^2-(\lambda^2+\Delta)w]$. To continue (16') above the second threshold, we deform the w and u contours in a way consistent with the $+i\epsilon$ prescription on s. The resulting contour integrals are performed numerically on a computer.

To continue (17) above threshold, we carry out the integration and analytically continue the resulting hypergeometric function above threshold to obtain

$$K_P(\beta)=\frac{\pi s^{\alpha+1/2}(i-\tan\pi\alpha)}{\Gamma(\alpha+\frac{3}{2})(\lambda^2+s)^\beta}-\frac{\Gamma(\beta-\alpha-\frac{3}{2})}{\Gamma(\beta)} \times\frac{F(1-\beta,1;\frac{5}{2}+\alpha-\beta;\lambda^2/(\lambda^2+s))}{(\lambda^2+s)(\lambda^2)^{\beta-\alpha-3/2}}. \quad (19)$$

As expected, there is just a single threshold in the potential-theory case.

The simplest way to solve (13) or (14) is to choose a value of s and then calculate G^2 as a function of α. The set of G^2-versus-α curves for different s is used to extract α as a function of s at constant G^2. Above threshold, α is complex and for a given s and Reα, Imα is varied to locate a real positive G^2. Changing Reα yields a new Imα and G^2. The Reα-versus-G^2 curves for various values of s are used to determine the trajectories. In practice, the trajectories are determined by a simple interpolation procedure on the University of Massachusetts time-sharing computer system.

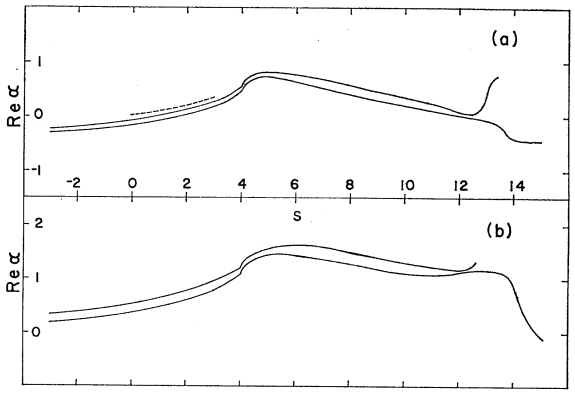

FIG. 5. Reα plotted as a function of s for the relativistic Regge trajectories calculated in the two approximations. In (a), $G^2=4.0$, while $G^2=16.0$ in (b). In both (a) and (b) the direct and exchange masses are given by $\lambda=\mu=1.0$, so that the elastic threshold is at $s=4.0$ and the four-particle threshold is at $s=16.0$. The dashed curve is from Chung and Snider (Ref. 6) for $G^2=3.4$. As in the potential-theory case, the lower solid curve is the first approximation, and the upper curve is the second approximation.

In Fig. 2, we plot the position of the potential-theory trajectory at $s=0$ as a function of the coupling constant g, where $G^2=g/2\sqrt{\pi}$. From these curves, comparing the exact and approximate solutions, we see that the approximate solutions are quantitatively correct up to $g=4$ and $\alpha(0)=0.25$, a long way from the domain where the weak-coupling solution $\alpha+1=g/2(-s)^{1/2}$ is valid. In Figs. 3 and 4, we show the potential-theory trajectories for $G^2=4$ and $G^2=16$ ($g=14$ and 64) in first and second approximations as well as the exact solution of Lovelace and Masson[8] for $g=7$. Note in the Reα-versus-s curves that the second approximation lies above the first approximation everywhere, but the two curves have essentially identical shape. Even though there is not quantitative agreement for these large couplings, the approximate trajectories have the same shape throughout the whole complex α plane. The agreement could be improved by decreasing the range of the potential (increasing λ). Since, in the units where $\hbar^2/2m=1$ (m being the mass of the scattering particles), the only mass in the problem is λ, increasing λ would alter the energy scale and effectively broaden the peak in the Reα-versus-s curve. The fact that the trajectories obtained from the relatively simple transcendental equation match the exact ones so closely gives us confidence in the validity of our method. The agreement between the first and second approximation also suggests that the finite-coupling trajectories extracted from perturbation theory in this manner are a good approximation to the exact solutions.

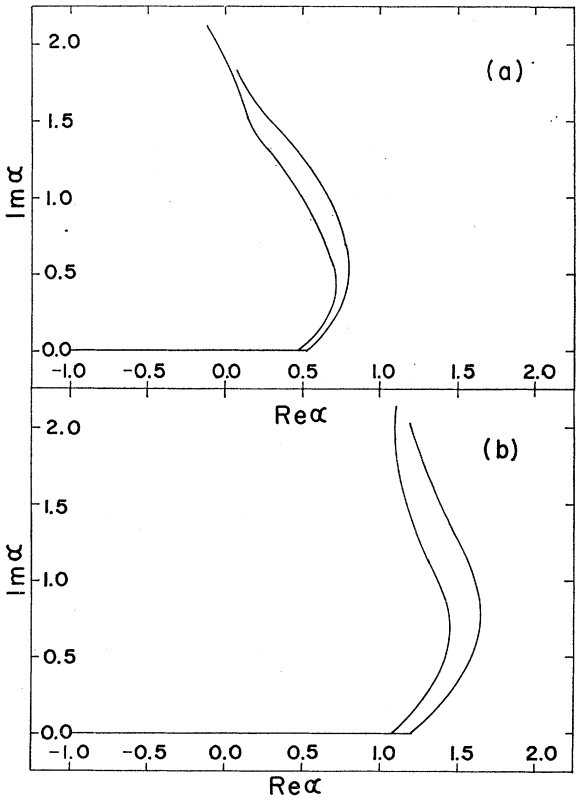

FIG. 6. The trajectories shown in Fig. 5 are drawn in the complex α plane. Again $G^2=4.0$ in (a) and 16.0 in (b) and both the first and second approximations are shown.

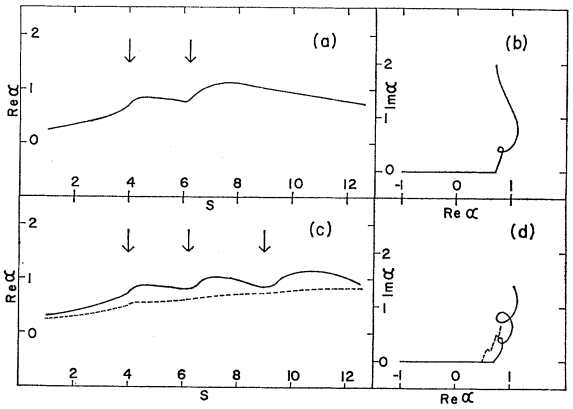

FIG. 7. In (a) the trajectory calculated in a two-threshold model is shown as a function of s, while in (b) it is drawn in the complex α plane. The exchange mass $\lambda=1.0$. The first threshold at $s=4\mu_1^2=4.0$ is coupled with a strength $G_1^2=4.0$. The second threshold at $s=4\mu_2^2=6.25$ is coupled with equal strength. In (c) and (d) the solid curve is a trajectory calculated in a three-threshold model. The channels are coupled with a strength $G_1^2=4.0$, $G_2^2=6.0$, and $G_3^2=8.0$, where $\mu_1=1.0$, $\mu_2=1.25$, and $\mu_3=1.5$. The exchange mass is given by $\lambda=1.0$. The dashed curve is the identical calculation with $\lambda=2.0$ in order to smooth out the local maxima in the curve of Reα versus s. In both (a) and (c) arrows mark the positions of the thresholds.

Figures 5 and 6 show the corresponding trajectories obtained from the field-theory model. Again the second approximation constitutes only a small correction. The only exact solution available is by Chung and Snider[6] and we show it also. The conclusion is that in the region below and just above the elastic threshold, relativistic trajectories are very similar to potential-theory ones, except for minor differences in scale and shape. However, as s approaches the second threshold at $4(\mu+\lambda)^2$, there are some distinctly relativistic effects. Depending on the value of G^2, Reα as a function of s stops falling and may even rise. This rise is followed by a sharp fall. Above the second threshold, Reα resumes its potential-like behavior and falls smoothly to -1. The relativistic trajectories make larger excursions into the complex plane, for comparable couplings, than do the potential-theory trajectories. We have not investigated the trajectories in great detail in the region of this second threshold. The accurate evaluation of the analytically continued double integral in (16′), while possible, is a time-consuming task; and it is not clear that the trajectories that would result warrant the effect, particularly in light of the approximations involved in the solution of (6). However, it is interesting to see, qualitatively, the effect of inelastic thresholds on Regge trajectories.

One new effect that can be explored with this simple ladder-diagram model is the effect of varying the masses in the problem. If the exchanged mass λ is increased for constant G^2 and direct-channel masses, the maximum value of Reα is depressed and the whole Reα-versus-s curve is flattened out. The scale of energy variation is

increased. If the exchanged mass is decreased, the peak becomes very sharp and the maximum value of Reα increases. If $\lambda=0$, Reα becomes infinite at threshold and we have the Coulomb limit of an infinite number of bound states. If G^2 and the exchange mass are held constant, while the direct mass 5 is increased to raise the threshold, we find that the trajectories always rise to threshold no matter how high it is. However, the maximum value of Reα is essentially unchanged. Raising the threshold energy just shifts the Reα-versus-s curves to the right.

As an application of our method we discuss a possible model for indefinitely rising trajectories. Chew[11] has suggested that such trajectories are generated by the continual opening of new channels. In this way, although each channel by itself produces a trajectory that turns over above threshold, the presence of new channels maintains the rising behavior. To examine such a model by our method, we note that N two-body channels are included in the theory by replacing the pair of propagators for the sides of the ladder by a weighted sum of N pairs of propagators. The final result is that in (13) or (14), $K(\beta)$ is replaced by $\sum G_i^2 K_i(\beta)$, where G_i^2 is the coupling strength to the ith channel whose threshold is at $s=4\mu_i^2$. $K_i(\beta)$ is given by (11) with μ^2 replaced by μ_i^2. In Fig. 7 we show trajectories from two- and three-threshold models. (We stay below the lowest inelastic threshold.) From the form of (13) it is easy to understand what is happening. The effects of the various channels are approximately additive in Reα. If each channel has equal strength, then each channel by itself would produce the same maximum value of Reα. Thus, unless the thresholds are very close together, they combine to produce a Reα that oscillates as a function of s and whose maximum value increases slightly, if at all. This roller-coaster effect is smoothed out by using the second approximation or by increasing the exchanged mass, but the model still does not generate a smoothly rising trajectory in the region where new thresholds are opening up. More interesting, though not shown in the figure, is the presence of stationary points in Imα as a function of s near the minima of Reα, even though in a single-threshold model Imα still rises smoothly in that region. If the higher thresholds have weaker strengths as suggested by experiment (i.e., more inelastic), then it is very hard to support a rising trajectory in this model. Although we have not considered all possible variations of the many parameters in this multiple threshold model, our conclusion is that it does not appear to be a plausible mechanism for generating rising trajectories. We note that such trajectories would always start at $\alpha=-1$. The mechanism which shifts $\alpha(-\infty)$ from -1 to $-\infty$ is probably responsible for the rise above threshold. On the other hand, multiparticle channels may be crucial for explaining physical trajectories.

Finally we comment on the validity of our method. From plots of G^2 versus α below threshold, it can be seen that at fixed s, there is a point where a large increase in G^2 produces a small change in the value of α obtained from (13). The exact calculations of Lovelace and Masson[8] tell us that α should continue to increase. Hence, for sufficiently strong couplings, (13) ceases to be valid. However, the fact that (14) gives larger values of α for the same G^2 suggests that including more correction terms would increase the region in which the method provides reliable results. The most encouraging feature of our solution is that the qualitative structure of the curves is correct. No one should try to make a detailed comparison with experiment with our theory. We also mention that although ladder diagrams contain three-particle cuts, the transcendental equation for α developed here does not have such cuts in its approximate form. However, it does have a nontrivial dependence on the exchange mass, which leads to a four-particle cut. Since ladder diagrams do not satisfy three-particle unitarity, the absence of three-particle cuts is not disturbing.

There are several possible applications of this general approach which come to mind. One involves changing the basic three-particle interaction from a field-theoretic point vertex to one involving form factors. Work is nearly complete on a class of models of this type. A second application would involve investigations of the first daughter trajectory; exact solutions like that given by (1) are available for secondary trajectories in ladder diagrams.[12] Such investigations might answer the question as to whether any of the secondary Regge poles reach the physical region along with the leading pole. A third application would involve realistic investigations of Regge-cut phenomena. Perturbation-theory models are the only ones in which cuts arising from third spectral functions are thoroughly understood.[13] However, the weak-coupling restriction has limited the usefulness of these models in physically interesting situations. Still another possible application would be to a model involving the exchange of an infinite set of particles. Such a theory would contain some of the features of the Veneziano model and might be considered one method of unitarizing it. Work is in progress on a model of this type.

---

[11] G. F. Chew, in Proceedings of the Regge-Pole Conference, University of California, Irvine, Calif., 1969 (unpublished).

[12] A. R. Swift, J. Math. Phys. **8**, 2420 (1967).

[13] S. Mandelstam, Nuovo Cimento **30**, 1148 (1963); J. C. Polkinghorne, J. Math. Phys. **4**, 1396 (1963).